

Perturbation Analysis of Learning Algorithms: A Unifying Perspective on Generation of Adversarial Examples

Emilio Rafael Balda, Arash Behboodi, and Rudolf Mathar*

December 19, 2018

Abstract

Despite the tremendous success of deep neural networks in various learning problems, it has been observed that adding an intentionally designed adversarial perturbation to inputs of these architectures leads to erroneous classification with high confidence in the prediction. In this work, we propose a general framework based on the perturbation analysis of learning algorithms which consists of convex programming and is able to recover many current adversarial attacks as special cases. The framework can be used to propose novel attacks against learning algorithms for classification and regression tasks under various new constraints with closed form solutions in many instances. In particular we derive new attacks against classification algorithms which are shown to achieve comparable performances to notable existing attacks. The framework is then used to generate adversarial perturbations for regression tasks which include single pixel and single subset attacks. By applying this method to autoencoding and image colorization tasks, it is shown that adversarial perturbations can effectively perturb the output of regression tasks as well.

1 Introduction

Deep Neural Networks (DNNs) excelled in recent years in many learning tasks and demonstrated outstanding achievements in speech analysis [HDY⁺12] and visual tasks [KSH12, HZRS16, SLJ⁺15, RHGS17]. Despite their success, they have been shown to suffer from instability in their classification under adversarial perturbations [SZS⁺14]. Adversarial perturbations are intentionally worst case designed noises that aim at changing the output of a DNN to an incorrect one. The explosion of research during past years makes it almost impossible to refer to all important works in this area and do justice to all excellent works. However, we refer to several important results from the literature, that are highly connected to this paper.

Although DNNs might achieve robustness to random noise [FMDF16], it was shown that there is a clear distinction between the robustness of a classifier to random noise and its robustness to adversarial perturbations. The existence of adversarial perturbations was known for machine learning algorithms [BNJT10], however, they were first noticed in deep learning research in [SZS⁺14]. The peculiarity of adversarial perturbations lied in the fact that they managed to fool state of the art networks into making confident and wrong decisions in classification tasks, and they, nevertheless, appeared unperceived to the naked eye. These discoveries gave rise to extensive research on understanding the instability of DNNs, exploring various attacks and devising multiple defenses (for instance refer to [AM18, WGQ17, FFF15] and references therein). Most adversarial attacks fall generally into two classes, white-box and black-box attacks. In white-box attacks, the attacker knows completely the architecture of the target algorithms and additionally, there

*Institute for Theoretical Information Technology (TI), RWTH Aachen University.

are attacks with partial knowledge of the architecture. However, black-box attacks require no information about the target neural network, see for instance [SBMC17]. In this work, the focus is on white-box attacks. The overall aim of attacks, as in [GSS14, MDFF16, RRN12], is to apply perturbations to the system inputs, that are not perceived by the system’s administrator, such that the performance of the system is severely degraded.

Adversarial perturbations were obtained in [SZS⁺14] to maximize the prediction error at the output and were approximated using box-constrained L-BFGS. The Fast Gradient Sign Method (FGSM) in [GSS14] was based on finding the scaled sign of the gradient of the cost function. Note that the FGSM aims at minimizing ℓ_∞ -norm of the perturbation while the former algorithm minimizes ℓ_2 -norm of the perturbation under box constraint on the perturbed example.

More effective attacks utilize either iterative procedures or randomizations. The algorithm DeepFool [MDFF16] conducts an iterative linearization of the DNN to generate perturbations that are minimal in the ℓ_p -norm for $p > 1$. In [KGB16] the authors propose an iterative version of FGSM, called Basic Iterative Method (BIM). This method was later extended in [MMS⁺18], where randomness was introduced in the computation of adversarial perturbations. This attack is called the Projected Gradient Descent (PGD) method and was employed in [MMS⁺18] to devise a defense against adversarial examples. An iterative algorithm based on PGD combined with randomization was introduced in [ACW18] and has been used to dismantle many defenses so far [AC18]. Another popular way of generating adversarial examples is by constraining the ℓ_0 -norm of the perturbation. These types of attacks are known as single pixel attacks [SVK17] and multiple pixel attacks [PMJ⁺16].

An interesting feature of these perturbations is their generalization over other datasets and DNNs [RRN12, GSS14]. These perturbations are called universal adversarial perturbations. This is partly explained by the fact that certain underlying properties of the perturbation, such as direction in case of image perturbation, matters the most and is therefore generalized through different datasets. For example, the attack from [TKP⁺18] shows that adversarial examples transfer from one random instance of a neural network to another. In that work, the authors showed the effectiveness of these types of attacks for enhancing the robustness of neural networks, since they provide diverse perturbations during adversarial training. Moreover, [MDFFF17] showed the existence of universal adversarial perturbations that are independent from the system and the target input.

Since the rise of adversarial examples for image classification, novel algorithms have been developed for attacking other types of systems. In the field of computer vision, [MKBF17] constructed an attack on image segmentation, while [XWZ⁺17] designed attacks for object detection. The Houdini attack [CANK17] aims at distorting speech recognition systems. Moreover, [PMSH16] tailored an attack for recurrent neural networks, and [LHL⁺17] for reinforcement learning. Adversarial examples exist for probabilistic methods as well. For instance, [KFS18] showed the existence of adversarial examples for generative models. For regression problems, [TTV16] designed an attack that specifically targets variational autoencoders.

There are various theories regarding the nature of adversarial examples and the subject is heavily investigated. Initially, the authors in [GSS14] proposed the linearity hypothesis where the existence of adversarial images is attributed to the approximate linearity of classifiers, although this hypothesis has been challenged in [TG16]. Some other theories focus mostly on decision boundaries of classifiers and their analytic properties [FMDF16, FMDF17]. The work from [RSL18] provides a framework for determining the robustness of a classifier against adversarial examples with some performance guarantees. For a more recent theoretical approach to this problem refer to [TSE⁺18].

There exist several types of defenses against adversarial examples, as well as subsequent methods for bypassing them. For instance, the authors in [CW17] proposed three attacks to bypass defensive distillation of the adversarial perturbations [PMW⁺16]. Moreover, the attacks from [ACW18], bypassed 7 out of 9 non-certified defenses of ICLR 2018 that claimed to be

white-box secure. The most common defense is adding adversarial examples to the training set, also known as adversarial training. For that purpose different adversarial attacks may be employed. Recently, the PGD attack is used in [MMS⁺18] to provide the state of the art defense against adversarial examples for various image classification datasets.

1.1 Our Contribution

In this work, we focus on the generation of adversarial examples with a sufficiently general framework that includes many existing attacks and can be easily extended to generate new attacks for different scenarios. We build upon our previous work [BBM18] to introduce a connection between perturbation analysis of learning algorithms and adversarial perturbations. This leads to a general formulation for the problem of generating adversarial examples using convex programming. The general framework includes many existing attacks as special cases, provides closed form solutions and can be easily extended to generate new algorithms. In particular, we derive novel algorithms for designing adversarial attacks for classification which are benchmarked with state of the art attacks.

Another contribution of this paper is to employ this framework in context of adversarial perturbations for regression problems, a topic that has not been yet widely explored. Regression loss functions differ from classification loss functions in that it is sufficient to maximize the output perturbation, for instance measured in ℓ_2 -norm. In classification tasks, such a maximization might not necessarily change the output label particularly because these perturbations might push the instances far away from classification margins. There is no natural margin in regression tasks. We address various technical difficulties of this problem and use our framework to generate adversarial examples for regression tasks. In particular single pixel and single subset attacks are discussed. It is shown that this problem is related to the MaxCut problem and hence difficult to solve. We propose a greedy algorithm to overcome this issue.

Finally, the proposed algorithms are experimentally evaluated using state of the art benchmarks for classification and regression tasks. It is shown that our proposed method achieves comparable and sometimes better performance than many existing attacks for classification problems. Furthermore, it is shown that regression tasks such as image colorization and autoencoding suffer from adversarial perturbations as well.

2 Fooling Classifiers with First-Order Perturbation Analysis

The perturbation analysis, also called sensitivity analysis, is used in signal processing for analytically quantifying the error at the output of a system that occurs as consequence of a known perturbation at the system’s input. Adversarial images can also be considered as a slightly perturbed version of original images that manage to change the output of the classifier. Indeed, the generation of adversarial examples in [MDFF16, GSS14] is implicitly based on maximizing the effect of an input perturbation on a relevant function which is either the classifier function or the cost function used for training. In the FGSM, given in [GSS14], the perturbation at the output of the training cost function is first analyzed using first-order perturbation analysis of the cost function and then maximized to fool the algorithm. The DeepFool method, given in [MDFF16], maximizes the output perturbation for the linearized approximation of the underlying classifier which is indeed its first order-perturbation analysis. We develop further the connection between perturbation analysis and adversarial examples in this section.

2.1 Adversarial Perturbation Design

As it was mentioned above, adversarial examples can be considered as perturbed version of training examples by an adversarial perturbation $\boldsymbol{\eta}$. The perturbation analysis of classifiers is particularly difficult in general since the classifier function maps inputs to discrete set of labels

and therefore it is not differentiable. Instead, the classification problem is slightly modified as follows.

Definition 1 (Classification). *A classifier is defined by the mapping $k : \mathbb{R}^M \rightarrow [K]^1$ that maps an input $\mathbf{x} \in \mathbb{R}^M$ to its estimated class $k(\mathbf{x}) \in [K]$. The mapping $k(\cdot)$ is itself defined by*

$$k(\mathbf{x}) = \operatorname{argmax}_{l \in [K]} \{f_l(\mathbf{x})\}, \quad (1)$$

where $f_l(\mathbf{x}) : \mathbb{R}^M \rightarrow \mathbb{R}$'s are called score functions representing the probability of class belonging.

The function $f(\mathbf{x})$ given by the vector $(f_1(\mathbf{x}), \dots, f_m(\mathbf{x}))$ can be assumed to be differentiable almost everywhere for many classifiers.

The problem of adversarial generation consists of finding a perturbation that changes the classifier's output. However, it is desirable for adversarial perturbations to modify training instances only in an insignificant and unnoticeable way. This is controlled by adding a constraint on the adversarial perturbation. For instance, the perturbation generated by the FGSM is bounded in the ℓ_∞ -norm and the DeepFool method directly minimizes the norm of the perturbation that changes the classifier's output. While DeepFool might generate perturbations that are perceptible, the FGSM might not change the classifier's output.

An intriguing property of adversarial examples is that the perturbation does not distort the image significantly so that the naked eye can not detect any notable change in the images. One way of imposing this property in adversarial design is to constrain the input perturbation to keep the output of the ground truth classifier, also called oracle classifier [WGQ17], intact. The oracle classifier represents the naked eye in case of image classification. The score functions of the oracle classifier are denoted by $g_l(\cdot)$. The undetectability constraint for an adversarial perturbation $\boldsymbol{\eta}$ is formulated as

$$L_g(\mathbf{x}, \boldsymbol{\eta}) = g_{k(\mathbf{x})}(\mathbf{x} + \boldsymbol{\eta}) - \max_{l \neq k(\mathbf{x})} g_l(\mathbf{x} + \boldsymbol{\eta}) > 0. \quad (2)$$

Therefore the problem of adversarial design can be formulated as follows.

Problem 1 (Adversarial Generation Problem). *For a given $\mathbf{x} \in \mathbb{R}^M$, find a perturbation $\boldsymbol{\eta} \in \mathbb{R}^M$ to fool the classifier $k(\cdot)$ by the adversarial sample $\hat{\mathbf{x}} = \mathbf{x} + \boldsymbol{\eta}$ such that $k(\mathbf{x}) \neq k(\hat{\mathbf{x}})$ and the oracle classifier is not changed, i.e.,*

$$\begin{aligned} \text{Find : } & \boldsymbol{\eta} \\ \text{s.t. } & L_f(\mathbf{x}, \boldsymbol{\eta}) = f_{k(\mathbf{x})}(\mathbf{x} + \boldsymbol{\eta}) - \max_{l \neq k(\mathbf{x})} f_l(\mathbf{x} + \boldsymbol{\eta}) < 0 \\ & L_g(\mathbf{x}, \boldsymbol{\eta}) = g_{k(\mathbf{x})}(\mathbf{x} + \boldsymbol{\eta}) - \max_{l \neq k(\mathbf{x})} g_l(\mathbf{x} + \boldsymbol{\eta}) > 0 \end{aligned} \quad (\text{AGP})$$

The problem (AGP) is too general to be useful in practice directly. Next we explore different methods for making this problem tractable in some cases of interest. Since \mathbf{x} and f are fixed for the attacker, we simplify the notation by dropping the subscript f and assuming that gradients are always with respect to $\boldsymbol{\eta}$, that is $L(\mathbf{x}, \cdot) = L_f(\mathbf{x}, \cdot)$ and $\nabla L(\mathbf{x}, \cdot) = \nabla_{\boldsymbol{\eta}} L_f(\mathbf{x}, \cdot)$. We keep these shorthand notations throughout the paper.

2.2 Perturbation Analysis

There are two problems with the above formulation. First, the oracle function is not known in general and second the function $L(\mathbf{x}, \cdot)$ can be non-convex. One solution is to approximate $L(\mathbf{x}, \cdot)$ with a tractable function like linear functions which can be obtained through perturbation analysis of each individual function. The constraint on the oracle function can also be replaced

¹We denote the set $\{1, \dots, n\}$ by $[n]$ for $n \in \mathbb{N}$.

with constraints on the perturbation itself, for instance by imposing upper bounds on the ℓ_p -norm of the perturbation. Different classes of attacks can be obtained for different choices of p and are well known in the literature such as ℓ_∞ -attacks, ℓ_2 -attacks and ℓ_1 -attacks (see the survey in [AM18] for details).

The first order perturbation analysis of L yields

$$L(\mathbf{x}, \boldsymbol{\eta}) = L(\mathbf{x}, \mathbf{0}) + \boldsymbol{\eta}^\top \nabla L(\mathbf{x}, \mathbf{0}) + \mathcal{O}(\|\boldsymbol{\eta}\|_2^2),$$

where $\mathcal{O}(\|\boldsymbol{\eta}\|_2^2)$ contains higher order terms. The condition that corresponds to the oracle function can be approximated by $\|\boldsymbol{\eta}\|_p \leq \varepsilon$ for sufficiently small $\varepsilon \in \mathbb{R}^+$. This means that the noise is sufficiently small in ℓ_p -norm sense so that the observer does not notice it. These gradient and norm relaxations yield the following alternative optimization problem

$$\begin{aligned} \text{Find: } & \boldsymbol{\eta} \\ \text{s.t. } & L(\mathbf{x}, \mathbf{0}) + \boldsymbol{\eta}^\top \nabla L(\mathbf{x}, \mathbf{0}) < 0, \quad \|\boldsymbol{\eta}\|_p \leq \varepsilon. \end{aligned} \quad (3)$$

The above problem was also derived in [HA17] and is a convex optimization problem that can be efficiently solved. As we will see later, this formulation of the problem can be relaxed into some well known existing adversarial methods. However it is interesting to observe that this problem is not always feasible as stated in the following proposition.

Theorem 1. *The optimization problem (3) is not feasible if for $q = \frac{p}{p-1}$*

$$\varepsilon \|\nabla L(\mathbf{x}, \mathbf{0})\|_q < L(\mathbf{x}, \mathbf{0}). \quad (4)$$

Proof. The proof follows a simple duality argument and is an elementary optimization theory result. A similar result can be inferred from [HA17]. We repeat the proof for completeness. Note that the dual norm of ℓ_p is defined by

$$\|\mathbf{x}\|_p^* = \sup\{\mathbf{a}^\top \mathbf{x} : \|\mathbf{a}\|_p \leq 1\}.$$

Furthermore $\|\mathbf{x}\|_p^* = \|\mathbf{x}\|_q$ for $q = \frac{p}{p-1}$. Since the ℓ_p -norm of $\boldsymbol{\eta}$ is bounded by ε , the value of $\boldsymbol{\eta}^\top \nabla L(\mathbf{x}, \mathbf{0})$ is always bigger than $-\varepsilon \|\nabla L(\mathbf{x}, \mathbf{0})\|_p^*$. However if the condition (4) holds, then we have

$$L(\mathbf{x}, \mathbf{0}) + \boldsymbol{\eta}^\top \nabla L(\mathbf{x}, \mathbf{0}) \geq L(\mathbf{x}, \mathbf{0}) - \varepsilon \|\nabla L(\mathbf{x}, \mathbf{0})\|_p^* > 0.$$

Therefore, the problem is not feasible. \square

Theorem 1 shows that given a vector \mathbf{x} , the adversarial perturbation should have at least ℓ_p -norm equal to $\frac{L(\mathbf{x}, \mathbf{0})}{\|\nabla L(\mathbf{x}, \mathbf{0})\|_q}$. In other words if the ratio $\frac{L(\mathbf{x}, \mathbf{0})}{\|\nabla L(\mathbf{x}, \mathbf{0})\|_q}$ is small, then it is easier to fool the network by the ℓ_p -attacks. In that sense, Theorem 1 provides an insight into the stability of classifiers. In [MDFF16], the authors suggest that the robustness of the classifiers can be measured as

$$\hat{\rho}_1(f) = \frac{1}{|\mathcal{D}|} \sum_{\mathbf{x} \in \mathcal{D}} \frac{\|\hat{\mathbf{r}}(\mathbf{x})\|_p}{\|\mathbf{x}\|_p},$$

where \mathcal{D} denotes the test set and $\hat{\mathbf{r}}(\mathbf{x})$ is the minimum perturbation required to change the classifier's output. The above theorem suggests that one can also use the following as the measure of robustness

$$\hat{\rho}_2(f) = \frac{1}{|\mathcal{D}|} \sum_{\mathbf{x} \in \mathcal{D}} \frac{L(\mathbf{x}, \mathbf{0})}{\|\nabla L(\mathbf{x}, \mathbf{0})\|_q}.$$

The lower $\hat{\rho}_2(f)$, the easier it gets to fool the classifier and therefore it becomes less robust to adversarial examples. One can also look at other statistics related to $\frac{L(\mathbf{x}, \mathbf{0})}{\|\nabla L(\mathbf{x}, \mathbf{0})\|_q}$ in order to evaluate the robustness of classifiers.

Theorem 1 shows that the optimization problem (3) might not be feasible. We propose to get around this issue by solving an optimization problem which keeps only one of the constraints, depending on the scenario, and selects an appropriate the objective function to preserve the other constraint as much as possible. The objective function in this sense models the deviation from the constraint and is minimized in the optimization problem. We consider two optimization problems for this purpose.

First, the norm-constraint on the perturbation is preserved. The following optimization problem, called gradient-based norm-constrained method (GNM), aims at minimizing $L(\mathbf{x}, \mathbf{0}) + \boldsymbol{\eta}^T \nabla L(\mathbf{x}, \mathbf{0})$ by solving the following problem:

$$\min_{\boldsymbol{\eta}} \{L(\mathbf{x}, \mathbf{0}) + \boldsymbol{\eta}^T \nabla L(\mathbf{x}, \mathbf{0})\} \quad \text{s.t.} \quad \|\boldsymbol{\eta}\|_p \leq \varepsilon. \quad (5)$$

This method finds the best perturbation under the norm-constraint. The constraint aims at guaranteeing that the adversarial images are still imperceptible by an ordinary observer. Note that (5) is fundamentally different from [MDFF16, HA17], where the norm of the noise does not appear as a constraint. Using a similar duality argument, the problem (5) has a closed form solution given below.

Theorem 2. *If $\nabla L(\mathbf{x}, \boldsymbol{\eta}) = (\frac{\partial L(\mathbf{x}, \boldsymbol{\eta})}{\partial \eta_1}, \dots, \frac{\partial L(\mathbf{x}, \boldsymbol{\eta})}{\partial \eta_M})$, the closed form solution to the minimizer of the problem (5) is given by*

$$\boldsymbol{\eta} = -\varepsilon \frac{1}{\|\nabla L(\mathbf{x}, \mathbf{0})\|_q^{q-1}} \text{sign}(\nabla L(\mathbf{x}, \mathbf{0})) \odot |\nabla L(\mathbf{x}, \mathbf{0})|^{q-1} \quad (6)$$

for $q = \frac{p}{p-1}$, where $\text{sign}(\cdot)$ and $|\cdot|^{q-1}$ are applied element-wise, and \odot denotes the element-wise (Hadamard) product. Particularly for $p = \infty$, we have $q = 1$ and the solution is given by the following

$$\boldsymbol{\eta} = -\varepsilon \text{sign}(\nabla L(\mathbf{x}, \mathbf{0})). \quad (7)$$

Proof. Based on the duality argument from convex analysis, it is known that

$$\sup_{\|\boldsymbol{\eta}\|_p \leq 1} \boldsymbol{\eta}^T \nabla L(\mathbf{x}, \mathbf{0}) = \|\nabla L(\mathbf{x}, \mathbf{0})\|_p^*,$$

where $\|\cdot\|^*$ is the dual norm. This implies that the objective function is lower bounded by $L(\mathbf{x}, \mathbf{0}) - \varepsilon \|\nabla L(\mathbf{x}, \mathbf{0})\|_p^*$. It is easy to verify that the minimum is attained by (6). \square

The advantage of (5), apart from being convex and enjoying computationally efficient solutions, is that one can incorporate other convex constraints into the optimization problem to guarantee additional required properties of the perturbation. Note that the introduced method in (5) can also be used for other target functions or learning problems. If the training cost function is maximized under a norm constraint, as in [GSS14], the solution of (5) with $p = \infty$ recovers the adversarial perturbations obtained via the FGSM. The problem (5) guarantees that the perturbation is small, however, it might not change the classifier's output.

The second optimization problem, on the other hand, preserves the constraint for changing the classifier's output and minimizes the perturbation norm instead. The feasibility problem of (3) can therefore be simplified to

$$\min_{\boldsymbol{\eta}} \|\boldsymbol{\eta}\|_p \quad \text{s.t.} \quad L(\mathbf{x}, \mathbf{0}) + \boldsymbol{\eta}^T \nabla L(\mathbf{x}, \mathbf{0}) \leq 0, \quad (8)$$

which recovers the result in [MDFF16] although without the iterative procedure. This problem has a similar closed form solution.

Proposition 1. If $\nabla L(\mathbf{x}, \boldsymbol{\eta}) = (\frac{\partial L(\mathbf{x}, \boldsymbol{\eta})}{\partial \eta_1}, \dots, \frac{\partial L(\mathbf{x}, \boldsymbol{\eta})}{\partial \eta_M})$, the closed form solution to the problem (8) is given by

$$\boldsymbol{\eta} = -\frac{L(\mathbf{x}, \mathbf{0})}{\|\nabla L(\mathbf{x}, \mathbf{0})\|_q^{q-1}} \text{sign}(\nabla L(\mathbf{x}, \mathbf{0})) \odot |\nabla L(\mathbf{x}, \mathbf{0})|^{q-1} \quad (9)$$

for $q = \frac{p}{p-1}$.

Note that the perturbation found in Proposition 1, like the solution to GNM, aligns with the gradient of the classifier function and they only differ in their norm. Although the perturbation in (9), unlike the solution to GNM, is able to fool the classifier, the perturbation in (9) might be perceptible by the oracle classifier. There are other variants of adversarial generation methods that rely on an implicit perturbation analysis of a relevant function. These methods can be easily obtained by small modification of the methods above.

Iterative procedures can be easily adapted to the current formulation by repeating the optimization problem until the classifier output changes while keeping the perturbation small at each step. Later we provide an iterative version of the GNM and compare it with DeepFool [MDF16], as well as other methods.

Another class of methods relies on introducing randomness in the generation process. A notable example is the PGD attack introduced in [MMS⁺18] which is one of the state of the art attacks. The first-order approximation is then taken around another point $\tilde{\boldsymbol{\eta}}$ with $\tilde{\varepsilon} \triangleq \|\tilde{\boldsymbol{\eta}}\|_p \leq \varepsilon$. In other words we approximate $L(\mathbf{x}, \cdot)$ by a linear function around the point $\tilde{\boldsymbol{\eta}}$ within an $\tilde{\varepsilon}$ -radius from $\boldsymbol{\eta} = \mathbf{0}$. This new point $\tilde{\boldsymbol{\eta}}$ can be computed at random using arbitrary distributions with ℓ_p -norm bounded by ε . Changing the center of the first order approximation from $\mathbf{0}$ to $\tilde{\boldsymbol{\eta}}$ does not change the nature of the problem since $L(\mathbf{x}, \boldsymbol{\eta}) \approx L(\mathbf{x}, \tilde{\boldsymbol{\eta}}) + (\boldsymbol{\eta} - \tilde{\boldsymbol{\eta}})^T \nabla L(\mathbf{x}, \tilde{\boldsymbol{\eta}})$ leads to the following problem

$$\min_{\boldsymbol{\eta}} L(\mathbf{x}, \tilde{\boldsymbol{\eta}}) + (\boldsymbol{\eta} - \tilde{\boldsymbol{\eta}})^T \nabla L(\mathbf{x}, \tilde{\boldsymbol{\eta}}) \quad \text{s.t.} \quad \|\boldsymbol{\eta}\|_p \leq \varepsilon,$$

which is equivalent to:

$$\min_{\boldsymbol{\eta}} \boldsymbol{\eta}^T \nabla L(\mathbf{x}, \tilde{\boldsymbol{\eta}}) \quad \text{s.t.} \quad \|\boldsymbol{\eta}\|_p \leq \varepsilon. \quad (10)$$

From this result one can add randomness to the computation of adversarial examples by selecting $\tilde{\boldsymbol{\eta}}$ in a random fasion. This is desirable when training models with adversarial examples since it increases the diversity of the adversarial perturbations during training [TKP⁺18].

3 From Classification to Regression

In classical statistical learning theory, regression problems are defined in the following manner. Given $N \in \mathbb{N}$ samples $\{(\mathbf{x}_i, \mathbf{y}_i)\}_{i=1}^N$ drawn according to some unknown distribution $P_{X,Y}$, a regression model computes a function $f : \mathbb{R}^M \rightarrow \mathbb{R}^K$ that aims to minimize the expected loss $\mathbb{E}_P(\mathcal{L}(f(\mathbf{x}), \mathbf{y}))$, where $\mathcal{L} : \mathbb{R}^M \times \mathbb{R}^K \rightarrow \mathbb{R}$ is a function that measures the similarity between $f(\mathbf{x})$ and \mathbf{y} . While logarithmic losses are popular in classification problems, the squared loss $\mathcal{L}(f(\mathbf{x}), \mathbf{y}) = \|f(\mathbf{x}) - \mathbf{y}\|_2^2$ is mostly used for the general regression setting. For the sake of notation, given \mathbf{y} and f , let us redefine $L(\mathbf{x}, \boldsymbol{\eta})$ as $L(\mathbf{x}, \boldsymbol{\eta}) = \mathcal{L}(f(\mathbf{x} + \boldsymbol{\eta}), \mathbf{y})$.

For a given f , \mathbf{x} and \mathbf{y} , an adversarial attacker finds an additive perturbation vector $\boldsymbol{\eta}$ that is *imperceptible* to the administrator of the target system, while maximizing the loss of the perturbed input $L(\mathbf{x}, \boldsymbol{\eta})$ as

$$\max_{\boldsymbol{\eta}} L(\mathbf{x}, \boldsymbol{\eta}) \quad \text{s.t.} \quad \boldsymbol{\eta} \text{ is imperceptible.}$$

In contrast with classification problems where maximum perturbations at the output might not change the class, adversarial instances maximize the output perturbation in regression problems.

As in (5), a constraint on the ℓ_p -norm of $\boldsymbol{\eta}$ models imperceptibility leading to the following formulation of the problem

$$\max_{\boldsymbol{\eta}} \|\mathbf{y} - f(\mathbf{x} + \boldsymbol{\eta})\|_2^2 \quad \text{s.t.} \quad \|\boldsymbol{\eta}\|_p \leq \varepsilon. \quad (11)$$

Consider the image colorization problem where the goal is to add proper coloring on top of gray scale images. In this problem, $f(\cdot)$ is the regression algorithm and assumed to be known however the ground truth colorization \mathbf{y} is generally unknown. Without knowing \mathbf{y} , the optimization problem (11) is ill posed and cannot be solved in general. There are some cases where the output \mathbf{y} is known by the nature of the problem, for instance, when $f(\cdot)$ is an encoder-decoder pair as in autoencoders for which $\mathbf{y} = \mathbf{x}$.

Since the goal is to perturb the acting regression algorithm, we can assume that $\mathbf{y} \approx f(\mathbf{x})$ which means that the algorithm provides a good although not perfect approximation of the ground truth function. We use the formulation in (11) and discuss the implications of applying the approximation $\mathbf{y} \approx f(\mathbf{x})$ in later sections.

3.1 A Quadratic Programming Problem

In general $f(\mathbf{x})$ is a non-linear and non-convex function, so we have that $L(\mathbf{x}, \cdot)$ is non-convex. Here again the perturbation analysis of $f(\cdot)$ can be used to relax (11) and to obtain a convex formulation of the adversarial problem. The first order perturbation analysis of $f(\mathbf{x})$ yields the approximation $f(\mathbf{x} + \boldsymbol{\eta}) \approx f(\mathbf{x}) + \mathbf{J}_f(\mathbf{x})\boldsymbol{\eta}$, where $\mathbf{J}_f(\cdot)$ is the Jacobian matrix of $f(\cdot)$. This approximation leads to the following convex approximation of $L(\mathbf{x}, \cdot)$:

$$\begin{aligned} L(\mathbf{x}, \boldsymbol{\eta}) &\approx \|\mathbf{y}\|_2^2 - 2\mathbf{y}^T(f(\mathbf{x}) + \mathbf{J}_f(\mathbf{x})\boldsymbol{\eta}) + \|f(\mathbf{x}) + \mathbf{J}_f(\mathbf{x})\boldsymbol{\eta}\|_2^2 \\ &= \|\mathbf{y}\|_2^2 - 2\mathbf{y}^T f(\mathbf{x}) + \|f(\mathbf{x})\|_2^2 \\ &\quad + 2(f(\mathbf{x}) - \mathbf{y})^T \mathbf{J}_f(\mathbf{x})\boldsymbol{\eta} + \|\mathbf{J}_f(\mathbf{x})\boldsymbol{\eta}\|_2^2. \end{aligned}$$

Since the first three terms of this expression do not depend on $\boldsymbol{\eta}$, the optimization problem from (11) is reduced to

$$\max_{\boldsymbol{\eta}} 2(f(\mathbf{x}) - \mathbf{y})^T \mathbf{J}_f(\mathbf{x})\boldsymbol{\eta} + \|\mathbf{J}_f(\mathbf{x})\boldsymbol{\eta}\|_2^2 \quad \text{s.t.} \quad \|\boldsymbol{\eta}\|_p \leq \varepsilon. \quad (12)$$

The above convex maximization problem is, in general, challenging and NP-hard. Nevertheless, since \mathbf{y} is usually not known, we may use the assumption that $\mathbf{y} \approx f(\mathbf{x})$, which simplifies the problem to

$$\max_{\boldsymbol{\eta}} \|\mathbf{J}_f(\mathbf{x})\boldsymbol{\eta}\|_2^2 \quad \text{s.t.} \quad \|\boldsymbol{\eta}\|_p \leq \varepsilon. \quad (13)$$

Although this problem is a convex quadratic maximization under an ℓ_p -norm constraint and in general challenging, it can be solved efficiently in some cases. For general p , the maximum value is indeed related to the operator norm of $\mathbf{J}_f(\mathbf{x})$ [HJ13]. This norm is central in stability analysis of many signal processing algorithms (for instance see [FR13]). The operator norm of a matrix $\mathbf{A} \in \mathbb{C}^{m \times n}$ between ℓ_p and ℓ_q is defined as

$$\|\mathbf{A}\|_{p \rightarrow q} \triangleq \sup_{\|\mathbf{x}\|_p \leq 1} \|\mathbf{A}\mathbf{x}\|_q.$$

Using this notion, we can see that $\|\frac{\boldsymbol{\eta}}{\varepsilon}\|_p \leq 1$ leads to $\|\mathbf{J}_f(\mathbf{x})\boldsymbol{\eta}\|_2 = \varepsilon \|\mathbf{J}_f(\mathbf{x})\frac{\boldsymbol{\eta}}{\varepsilon}\|_2 \leq \varepsilon \|\mathbf{J}_f(\mathbf{x})\|_{p \rightarrow 2}$. Therefore, the problem of finding a solution to (13) amounts to finding the operator norm $\|\mathbf{J}_f(\mathbf{x})\|_{p \rightarrow 2}$. First observe that the maximum value is achieved on the border namely for

$\|\boldsymbol{\eta}\|_p = \varepsilon$. In the case where $p = 2$, this problem has a closed-form solution. If \mathbf{v}_{\max} is the unit ℓ_2 -norm eigenvector corresponding to the maximum eigenvalue of $\mathbf{J}_f(\mathbf{x})^T \mathbf{J}_f(\mathbf{x})$, then

$$\boldsymbol{\eta}^* = \pm \varepsilon \mathbf{v}_{\max} \quad (14)$$

solves the optimization problem. The maximum eigenvalue of $\mathbf{J}_f(\mathbf{x})^T \mathbf{J}_f(\mathbf{x})$ corresponds to the square of the spectral norm $\|\mathbf{J}_f(\mathbf{x})\|_{2 \rightarrow 2}$.

Another interesting case is when $p = 1$. In general, the ℓ_1 -norm is usually used as a regularization technique to promote sparsity. When the solution of a problem should satisfy a sparsity constraint, the direct introduction of this constraint into the optimization leads to NP-hardness of the problem. Instead the constraint is relaxed by adding ℓ_1 -norm regularization. The adversarial perturbation designed in this way tends to have only a few non-zero entries. This corresponds to scenarios like single pixel attacks where only a few pixels are supposed to change. For this choice, we have

$$\|\mathbf{A}\|_{1 \rightarrow 2} = \max_{k \in [n]} \|\mathbf{a}_k\|_2,$$

where \mathbf{a}_k 's are the columns of \mathbf{A} . Therefore, if the columns of the Jacobian matrix are given by $\mathbf{J}_f(\mathbf{x}) = [\mathbf{J}_1 \dots \mathbf{J}_M]$, then

$$\|\mathbf{J}_f(\mathbf{x})\boldsymbol{\eta}\|_2 \leq \varepsilon \max_{k \in [M]} \|\mathbf{J}_k\|_2,$$

and the maximum is attained with

$$\boldsymbol{\eta}^* = \pm \varepsilon \mathbf{e}_{k^*} \quad \text{for} \quad k^* = \operatorname{argmax}_{k \in [M]} \|\mathbf{J}_k\|_2, \quad (15)$$

where the vector \mathbf{e}_i is the i -th canonical vector. For the case of gray-scale images, where each pixel is represented by a single entry of \mathbf{x} , this constitutes a single pixel attack. Some additional constraints must be added in the case of RGB images, where each pixel is represented by a set of three values.

Finally, the case where the adversarial perturbation is bounded with the ℓ_∞ -norm is also of particular interest. This bound guarantees that the noise entries have bounded values. The problem of designing adversarial noise corresponds to finding $\|\mathbf{J}_f(\mathbf{x})\|_{\infty \rightarrow 2}$. Unfortunately, this problem turns out to be NP-hard [Roh00]. However, it is possible to approximate this norm using semi-definite programming as proposed in [HH15]. Semi-definite programming scales badly with input dimension in terms of computational complexity, namely $O(n^6)$ with n the underlying dimension, and therefore might not be suitable for fast generation of adversarial examples when the input dimension is very high. We address these problems later in Section 4, where we obtain fast approximate solutions for $\|\mathbf{J}_f(\mathbf{x})\|_{\infty \rightarrow 2}$ and single pixel attacks.

3.2 A Linear Programming Problem

The methods derived in Section 3.1 suffer from one main drawback, they require storing $\mathbf{J}_f(\mathbf{x}) \in \mathbb{R}^{K \times M}$ into memory. While this may be doable for some applications, it is not feasible for others. For example, if the target system is an autoencoder for RGB images with size 680×480 , that is $M = K = 680 \cdot 480 \cdot 3 \approx 9 \cdot 10^5$, storing $\mathbf{J}_f(\mathbf{x}) \in \mathbb{R}^{9 \cdot 10^5 \times 9 \cdot 10^5}$ requires loading around $8 \cdot 10^{11}$ values into memory, which is in most cases not tractable. Note that, in order to solve (13) for $p = 2$, we would require computing the eigenvalue decomposition of $\mathbf{J}_f(\mathbf{x})^T \mathbf{J}_f(\mathbf{x})$ as well. This motivates us to relax the problem into a linear programming problem as in Section 2, where $\mathbf{J}_f(\mathbf{x})$ is computed implicitly and we do not require to store it. To that end, we relax (11) by directly applying a first order approximation of L , that is $L(\mathbf{x}, \boldsymbol{\eta}) \approx L(\mathbf{x}, \mathbf{0}) + \boldsymbol{\eta}^T \nabla L(\mathbf{x}, \mathbf{0})$. Using this approximation the problem from (11) is now simplified to

$$\max_{\boldsymbol{\eta}} \nabla L(\mathbf{x}, \mathbf{0})^T \boldsymbol{\eta} \quad \text{s.t.} \quad \|\boldsymbol{\eta}\|_p \leq \varepsilon, \quad (16)$$

where $\nabla L(\mathbf{x}, \mathbf{0}) = -2\mathbf{J}_f(\mathbf{x})^T (\mathbf{y} - f(\mathbf{x}))$. Note that the attacks discussed in Section 2 for classification follow the same formulation with another choice of $L(\mathbf{x}, \cdot)$. Therefore, the closed-form solution of (16) can be obtained from (6).

Unfortunately using $\mathbf{y} \approx f(\mathbf{x})$ yields zero gradient in (16), thus leaving this approximation useless for obtaining adversarial perturbations. This problem is tackled by taking the approximation around another random point $\tilde{\boldsymbol{\eta}}$ within an $\tilde{\varepsilon}$ -ball radius from $\boldsymbol{\eta} = \mathbf{0}$ as in (10), with $\tilde{\varepsilon} \leq \varepsilon$. As it was mentioned above, this dithering mechanism is also used in classification problems for instance in [MMS⁺18].

4 Single Subset Attacks

Another popular way of modeling undetectability, in the field of image recognition, is by constraining the number of pixels that can be modified by the attacker. This gave birth to single and multiple pixel attacks. Note that, for the case of gray-scale images, the solutions obtained in (15) and (6) provide already single pixels attacks. This is not true for RGB images where each pixel is represented by a subset of three values. Since our analysis is not limited to image based systems, we refer to these type of attacks which target only a subset of entries as single subset attacks.

Since perturbations belong to \mathbb{R}^M , let us partition $[M] = \{1, \dots, M\}$ into S possible subsets $\mathcal{S}_1, \dots, \mathcal{S}_S$. The sets can in general have different cardinalities. However, we assume here that all of them have the same cardinality of $Z = M/S$, where $\mathcal{S}_s = \{i_s^1, \dots, i_s^Z\} \subseteq [M]$. We define the mixed zero- \mathcal{S} norm $\|\cdot\|_{0,\mathcal{S}}$ of a vector, for the partition $\mathcal{S} = \{\mathcal{S}_1, \dots, \mathcal{S}_S\}$, as the number of subsets containing at least one index associated to a non-zero entry of \mathbf{x}^2 :

$$\|\mathbf{x}\|_{0,\mathcal{S}} = \sum_{i=1}^S \mathbf{1}(\|\mathbf{x}_{\mathcal{S}_i}\| \neq 0).$$

Therefore, $\|\boldsymbol{\eta}\|_{0,\mathcal{S}}$ counts the number of subsets modified by an attacker. To guarantee that only one subset is active, an additional constraint can be added to the optimization problem. This leads to the following formulation of the single subset attack for the regression problem.

$$\max_{\boldsymbol{\eta}} \|\mathbf{y} - f(\mathbf{x} + \boldsymbol{\eta})\|_2^2 \quad \text{s.t.} \quad \|\boldsymbol{\eta}\|_{\infty} \leq \varepsilon, \|\boldsymbol{\eta}\|_{0,\mathcal{S}} = 1. \quad (17)$$

A similar formulation holds as well for classification problems. The mixed norm $\|\cdot\|_{0,\mathcal{S}}$ is widely used in signal processing and compressed sensing to promoting group sparsity [RRN12].

4.1 Single Subset Attack for the Quadratic Problem

As in Section 3.1, the approximations $f(\mathbf{x} + \boldsymbol{\eta}) \approx f(\mathbf{x}) + \mathbf{J}_f(\mathbf{x})\boldsymbol{\eta}$ and $\mathbf{y} \approx f(\mathbf{x})$ simplify the problem (17) to

$$\max_{\boldsymbol{\eta}} \|\mathbf{J}_f(\mathbf{x})\boldsymbol{\eta}\|_2^2 \quad \text{s.t.} \quad \|\boldsymbol{\eta}\|_{\infty} \leq \varepsilon, \|\boldsymbol{\eta}\|_{0,\mathcal{S}} = 1. \quad (18)$$

As it was mentioned above, the problem is NP-hard without the mixed-norm constraint. We try to find an approximate solution to a simpler problem where only the set \mathcal{S}_s is to be modified by the attacker for $s \in [S]$. Finding the perturbation on this set amounts to solving the following problem:

$$\boldsymbol{\eta}_s = \underset{\boldsymbol{\eta}}{\operatorname{argmax}} \|\mathbf{J}_f(\mathbf{x})\boldsymbol{\eta}\|_2^2 \quad \text{s.t.} \quad \|\boldsymbol{\eta}\|_{\infty} \leq \varepsilon, (\boldsymbol{\eta})_{i_s^z} = 0 \quad \forall i_s^z \notin \mathcal{S}_s, \quad (19)$$

where $(\boldsymbol{\eta})_{i_s^z}$ denotes the i_s^z -th entry of $\boldsymbol{\eta}$. As discussed in Section 3.1, this problem is NP-hard. Since the maximization of a quadratic bowl over a box constraint lies in the corner points of the

²Similar to the so-called ℓ_0 -norm, this is not a proper norm.

feasible set, we have:

$$\boldsymbol{\eta}_s = \varepsilon \sum_{z=1}^Z \rho_{i_s^z}^* \mathbf{e}_{i_s^z}$$

with $\boldsymbol{\rho}_s^* \triangleq (\rho_{i_s^1}^*, \dots, \rho_{i_s^Z}^*)^\top \in \{-1, +1\}^Z$. The optimization problem can be equivalently formulated as follows:

$$\begin{aligned} \boldsymbol{\rho}_s^* &= \operatorname{argmax}_{\boldsymbol{\rho}_s \in \{-1, +1\}^Z} \left\| \mathbf{J}_f(\mathbf{x}) \left(\varepsilon \sum_{z=1}^Z \rho_{i_s^z} \mathbf{e}_{i_s^z} \right) \right\|_2^2 \\ &= \operatorname{argmax}_{\boldsymbol{\rho}_s \in \{-1, +1\}^Z} \sum_{z=1}^Z \sum_{w=1}^Z \rho_{i_s^z} \rho_{i_s^w} \mathbf{J}_{i_s^z}^\top \mathbf{J}_{i_s^w}, \end{aligned}$$

for $\boldsymbol{\rho}_s \triangleq (\rho_{i_s^1}, \dots, \rho_{i_s^Z})^\top \in \{-1, +1\}^Z$ and \mathbf{J}_k the k -th column of $\mathbf{J}_f(\mathbf{x})$. This problem is indeed related to the well known MaxCut problem introduced by [GW95]. The literature is abound with works on the MaxCut problem, the efficient solutions and their recovery guarantees. A common solution to this problem is a relaxation by a semi-definite programming problem. However, as we discussed semi-definite programming solvers scales badly with the input dimension. Therefore, in the spirit of obtaining fast and scalable approximate solutions, that can later be used to design adversarial perturbations through iterative approximations, we propose to obtain approximate solutions using a greedy approach. To that end, and without loss of generality, let us assume that for a given \mathcal{S}_s , the indices $i_s^1, \dots, i_s^Z \in \mathcal{S}_s$ are sorted such that $\|\mathbf{J}_{i_s^1}\|_2 \geq \dots \geq \|\mathbf{J}_{i_s^Z}\|_2$. An approximate solution for $\rho_{i_s^z}^*$ is calculated in a greedy manner by setting $\rho_{i_s^1}^* = 1$ and recursively calculating

$$\rho_{i_s^z}^* = \operatorname{sign} \left(\left(\sum_{j=1}^{z-1} \rho_{i_s^j}^* \mathbf{J}_{i_s^j} \right)^\top \mathbf{J}_{i_s^z} \right) \quad \forall z = 2, \dots, Z. \quad (20)$$

As for greedy algorithms, this solution is fast, however, there is no optimality guarantee for it. For the case where $S = 1$ and $S = M$, the expression (20) is an approximate solution for (13) under the ℓ_∞ -norm constraint on the perturbation (i.e., $p = \infty$).

This method provides an approximate solution to the problem for a given choice of \mathcal{S}_s . The solution to (18) can then be obtained by solving the following problem:

$$\boldsymbol{\eta}^* = \boldsymbol{\eta}_{s^*}, \quad (21)$$

$$\text{with } s^* = \operatorname{argmax}_s \|\mathbf{J}_f(\mathbf{x}) \boldsymbol{\eta}_s\|_2^2 \text{ and } \boldsymbol{\eta}_s = \varepsilon \sum_{z=1}^Z \rho_{i_s^z}^* \mathbf{e}_{i_s^z}$$

This is based on naive exhaustive research over the subsets which is tractable only when the number of subsets is small enough.

4.2 Single Subset Attack for the Linear Problem

Following the steps from Section 3.2, we make use of the approximation $L(\mathbf{x}, \boldsymbol{\eta}) \approx L(\mathbf{x}, \tilde{\boldsymbol{\eta}}) + (\boldsymbol{\eta} - \tilde{\boldsymbol{\eta}})^\top \nabla L(\mathbf{x}, \tilde{\boldsymbol{\eta}})$ which leads to the formulation of (17) as a linear programming problem

$$\max_{\boldsymbol{\eta}} \boldsymbol{\eta}^\top \nabla L(\mathbf{x}, \tilde{\boldsymbol{\eta}}) \quad \text{s.t.} \quad \|\boldsymbol{\eta}\|_\infty \leq \varepsilon, \|\boldsymbol{\eta}\|_{0,S} = 1. \quad (22)$$

In the same manner as Section 4.1, for a given subset \mathcal{S}_s we define $\boldsymbol{\eta}_s$ as in (19). For this linear problem that results in

$$\boldsymbol{\eta}_s = \operatorname{argmax}_{\boldsymbol{\eta}} \nabla L(\mathbf{x}, \tilde{\boldsymbol{\eta}})^\top \boldsymbol{\eta} \quad \text{s.t.} \quad \|\boldsymbol{\eta}\|_\infty \leq \varepsilon, (\boldsymbol{\eta})_{i_s^z} = 0 \quad \forall i_s^z \notin \mathcal{S}_s.$$

| Type of Attack | Relaxed Problem | Closed-Form Solution |
|------------------------|-----------------|---------------------------|
| ℓ_2 / ℓ_∞ | (16) | (14) / (21) $^\diamond$ |
| constrained | (13) | (6) \blacktriangledown |
| Single-Subset attack | (18) | (21) $^\diamond$ |
| | (22) | (23) \blacktriangledown |

Table 1: Summary of the obtained closed-form solutions. **Remarks:** (\blacktriangledown) valid for regression and classification, ($^\diamond$) only an approximate solution.

| Algorithm | Objective function L | Iterative | Dithering |
|--------------------------------|---|--------------|--------------|
| FGSM [GSS14] | cross-entropy | \times | \times |
| DeepFool [MDF16] | (2) with l chosen using $\hat{\rho}_1(f)$ | \checkmark | \times |
| BIM [KGB16] | cross-entropy | \checkmark | \times |
| PGD [MMS ⁺ 18] | cross-entropy | \checkmark | \checkmark |
| Ensemble [TKP ⁺ 18] | cross-entropy using another f | \checkmark | \times |
| Targeted | (2) with l fixed to the target | \checkmark | \checkmark |
| Ours | (2) | \checkmark | \checkmark |

Table 2: Recovering Existing Attacks in Classification using this Framework.

In contrast to the definition of $\boldsymbol{\eta}_s$ from (19), in this case we have a closed form solution for $\boldsymbol{\eta}_s$ as

$$\boldsymbol{\eta}_s = \varepsilon \sum_{z=1}^Z \text{sign}((\nabla L(\mathbf{x}, \tilde{\boldsymbol{\eta}}))_{i_z^z}) \mathbf{e}_{i_z^z},$$

which implies that $\nabla L(\mathbf{x}, \tilde{\boldsymbol{\eta}})^T \boldsymbol{\eta}_s = \sum_{z=1}^Z |(\nabla L(\mathbf{x}, \tilde{\boldsymbol{\eta}}))_{i_z^z}|$. Therefore, the linear problem for the single subset attack (22) has the closed form solution

$$\boldsymbol{\eta}^* = \boldsymbol{\eta}_{s^*}, \text{ with } s^* = \underset{s}{\text{argmax}} \sum_{z=1}^Z |(\nabla L(\mathbf{x}, \tilde{\boldsymbol{\eta}}))_{i_z^z}| \quad (23)$$

and $\boldsymbol{\eta}_s = \varepsilon \sum_{z=1}^Z \text{sign}((\nabla L(\mathbf{x}, \tilde{\boldsymbol{\eta}}))_{i_z^z}) \mathbf{e}_{i_z^z}$. This results are valid for classification as well when replacing L with $L(\mathbf{x}, \boldsymbol{\eta}) = -(f_{k(\mathbf{x})}(\mathbf{x} + \boldsymbol{\eta}) - \max_{l \neq k(\mathbf{x})} f_l(\mathbf{x} + \boldsymbol{\eta}))$.

5 Iterative Versions of the Linear Problem

In the previous sections we have formulated several variations of the problem of generating adversarial perturbations. These results are summarized in Table 1. In the same spirit as DeepFool, we make use of the obtained closed form solutions to design adversarial perturbations using iterative approximations. In Algorithm 1 an iterative method based on the linear problem (16) is introduced. This corresponds to a gradient ascent method for maximizing $L(\mathbf{x}, \boldsymbol{\eta})$ with a fixed number of iterations and steps of equal ℓ_p -norm.

While generalizing the results for (16) into a gradient ascent method is trivial, the same is not true for the quadratic problem (13). The main reason for this is that, using the approximation $\mathbf{y} \approx f(\mathbf{x})$, we were able to simplify (12) into (13) since $\mathbf{y} - f(\mathbf{x}) \approx \mathbf{0}$. For an iterative version of this solution we must successively approximate $f(\cdot)$ around different points $\tilde{\mathbf{x}}$, which leads to $\mathbf{y} - f(\tilde{\mathbf{x}}) \neq \mathbf{0}$ even if $\mathbf{y} = f(\mathbf{x})$. We leave the task of investigating alternatives for designing iterative methods with the results for (13) for future works, and in Section 6 show that the non-iterative solutions for this method are still competitive.

Finally, replacing line 5 of Algorithm 1 with

$$\boldsymbol{\eta}_t^* \leftarrow \underset{\boldsymbol{\eta}}{\text{argmax}} \boldsymbol{\eta}^T \nabla L(\mathbf{x}, \tilde{\boldsymbol{\eta}}_t) \text{ s.t. } \|\boldsymbol{\eta}\|_p \leq \varepsilon, \|\boldsymbol{\eta}\|_{0,S} = 1$$

Algorithm 1 Iterative extension for ℓ_p constrained methods.

input: $\mathbf{x}, f, T, \varepsilon, \tilde{\varepsilon}_1, \dots, \varepsilon_T$.

output: $\boldsymbol{\eta}^*$.

Initialize $\boldsymbol{\eta}_1 \leftarrow \mathbf{0}$.

for $t = 1, \dots, T$ **do**

$\tilde{\boldsymbol{\eta}}_t \leftarrow \boldsymbol{\eta}_t + \text{random}(\tilde{\varepsilon}_t)$

$\boldsymbol{\eta}_t^* \leftarrow \text{argmax}_{\boldsymbol{\eta}} \boldsymbol{\eta}^T \nabla L(\mathbf{x}, \tilde{\boldsymbol{\eta}}_t)$ s.t. $\|\boldsymbol{\eta}\|_p \leq \varepsilon/T$ (Table 1)

$\boldsymbol{\eta}_{t+1} \leftarrow \boldsymbol{\eta}_t + \boldsymbol{\eta}_t^*$

end for

return: $\boldsymbol{\eta}^* \leftarrow \boldsymbol{\eta}_T$

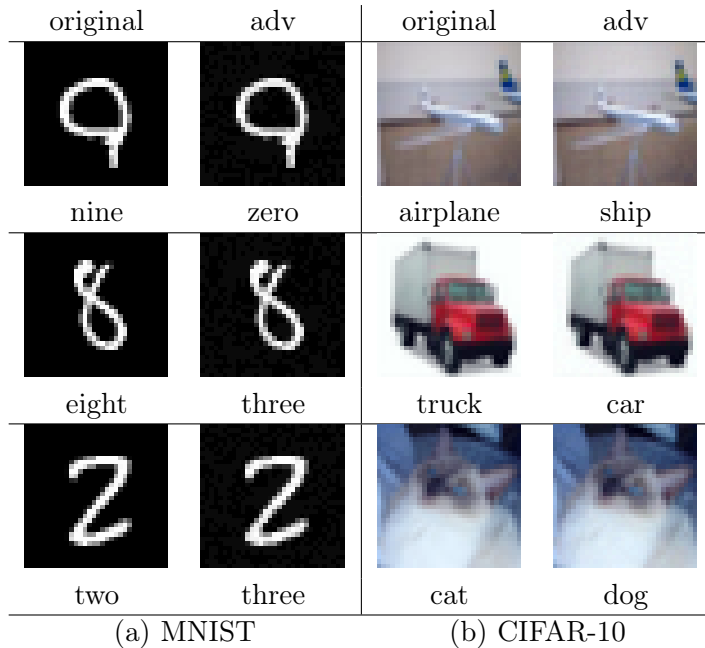


Figure 1: Examples of correctly classified images that are misclassified when adversarial noise is added using Algorithm 1.

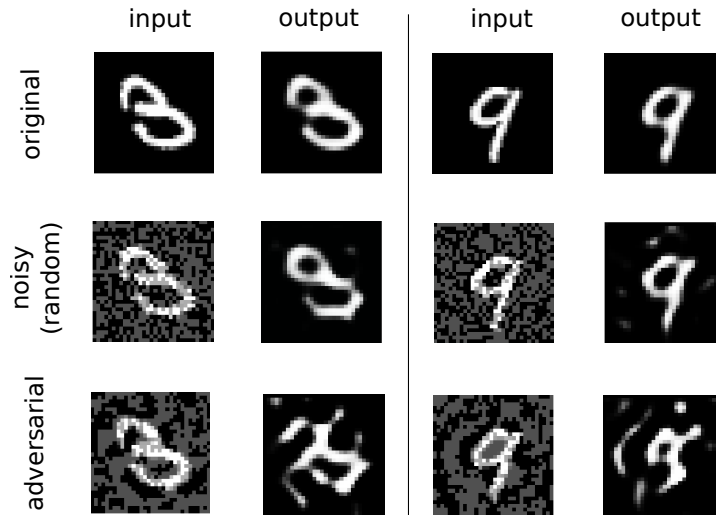
leads to a multiple subset attack, since we modify the values of one subset at every iteration. At every iteration, we may exclude the previously modified subsets from \mathcal{S} in order to ensure that a new subset is modified.

6 Experiments

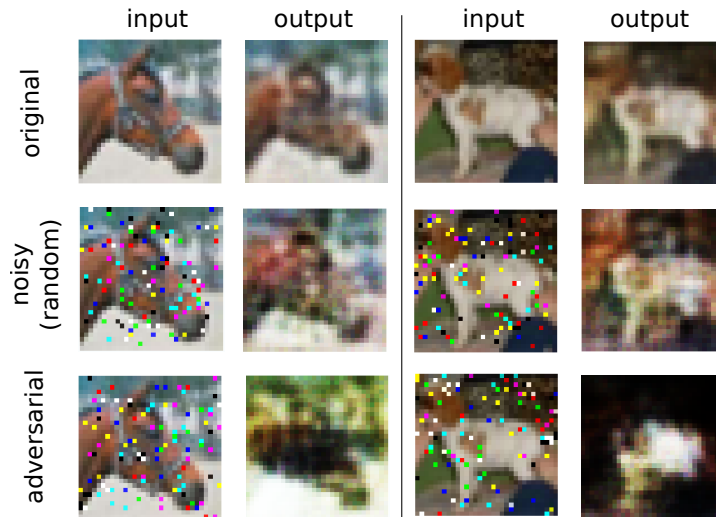
In this section, the proposed methods are used to fool neural networks in classification and regression problems. The goal of this section is twofold. First, we would like to examine the performance of the newly proposed attack in classification tasks, thereby showing the utility of current adversarial generation framework. Secondly we generate adversarial perturbations for regression tasks which only received small attention in the literature. For this purpose we use the MNIST [LCB10], CIFAR-10 [KH09], and STL-10 datasets.

6.1 Classification

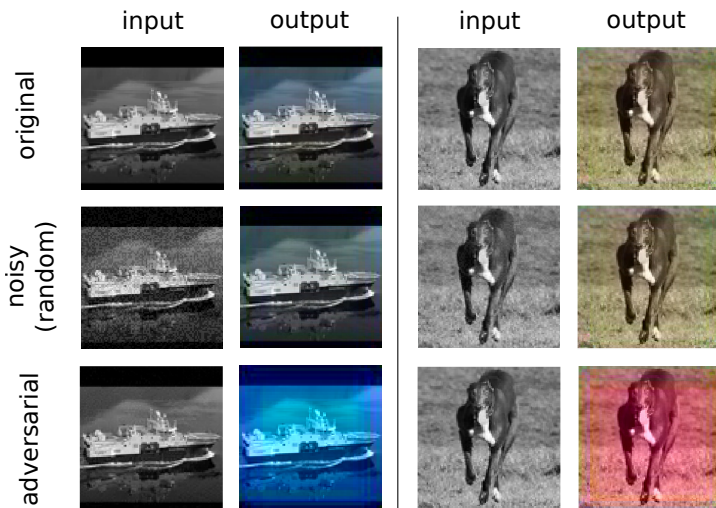
As discussed in Section 2, the appropriate loss function $L(\mathbf{x}, \boldsymbol{\eta})$ for image classification tasks that should be used in (5) is given by (AGP). For this problem, $\|\boldsymbol{\eta}\|_\infty \leq \varepsilon$ is a common constraint that models the undetectability, for sufficiently small ε , of adversarial noise by an observer.



(a) Autoencoder (96% compression)



(b) Autoencoder (50% compression)



(c) Image Colorization

Figure 2: Adversarial examples for (a): MNIST autoencoder obtained using $quadratic-\ell_\infty$, (b): CIFAR-10 autoencoder obtained using $linear-pixel-100$, (c): STL-10 colorization network obtained using $linear-\ell_\infty-20$.

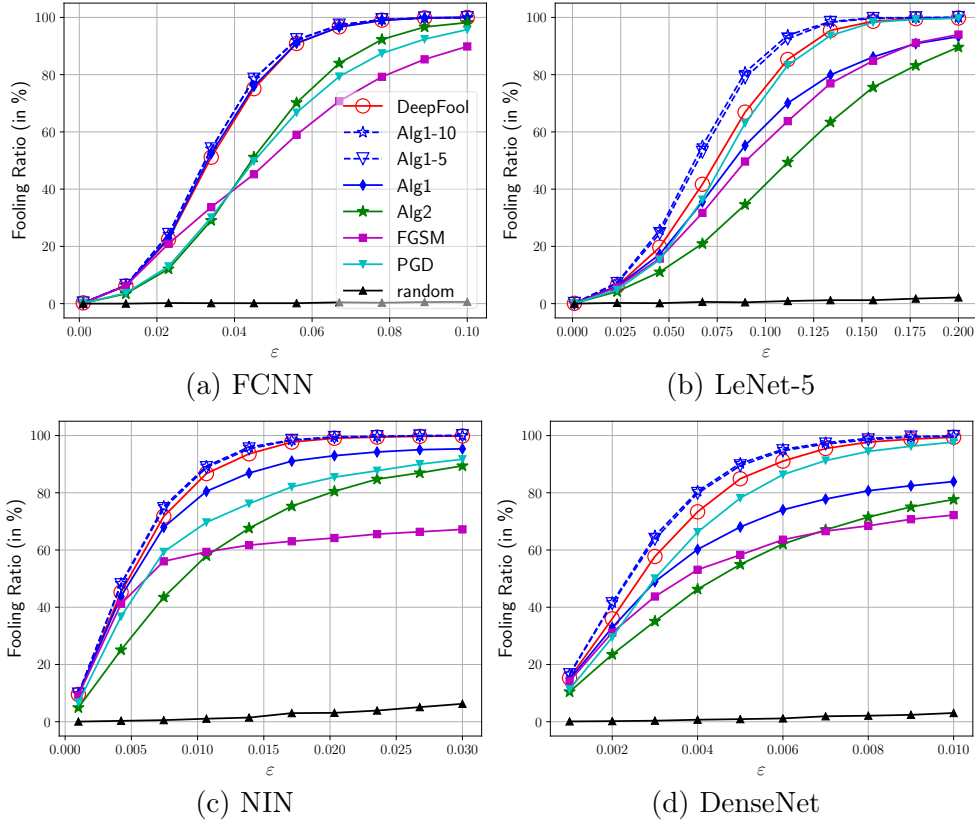


Figure 3: (a) and (b): Fooling ratio of the adversarial samples for different values of ϵ on the MNIST test dataset. (c) and (d): Fooling ratio of the adversarial samples for different values of ϵ on the CIFAR-10 test datasets.

However solving (5) involves finding the function $L(\mathbf{x}, \mathbf{0})$ which is defined as the minimum of $K - 1$ functions with K being the number of different classes. In large problems, this may significantly increase the computations required to fool one image. Therefore, we include a simplified version of this algorithm in our simulations. The non-iterative methods might not guarantee the fooling of the underlying network but on the other hand, the iterative methods might suffer from convergence problems.

To benchmark the proposed adversarial algorithms, we consider following methods tested on the aforementioned datasets:

- **Algorithm 1:** This algorithm solves (5) with $L(\mathbf{x}, \cdot)$ given by (AGP). Note that, for evaluating L at a given \mathbf{x} one must search over all $l \neq k(\mathbf{x})$. This can be computationally expensive when the number of possible classes (i.e., the number of possible values for l) is large. The ℓ_∞ -norm is chosen for the constraint. Moreover, an example of adversarial images obtained using this algorithm is shown in Figure 2.
- **Algorithm 1- T :** This is the iterative version of Algorithm 1 with T iterations. The adversarial perturbation is the sum of T perturbation vectors with ℓ_∞ -norm of ϵ/T computed through T successive approximations.
- **Algorithm 2:** This algorithm approximates (AGP) with $L(\mathbf{x}, \boldsymbol{\eta}) \approx f_{k(\mathbf{x})}(\mathbf{x} + \boldsymbol{\eta})$, thus reducing the computation of $L(\mathbf{x})$ when the number of classes is large. Note that we cannot use $L(\mathbf{x}, \boldsymbol{\eta}) < 0$ to guarantee that we have fooled the network. Nevertheless, the lower the value of $L(\mathbf{x}, \boldsymbol{\eta})$ the most likely it is that the network has been fooled. The same reasoning is valid for the FGSM algorithm.

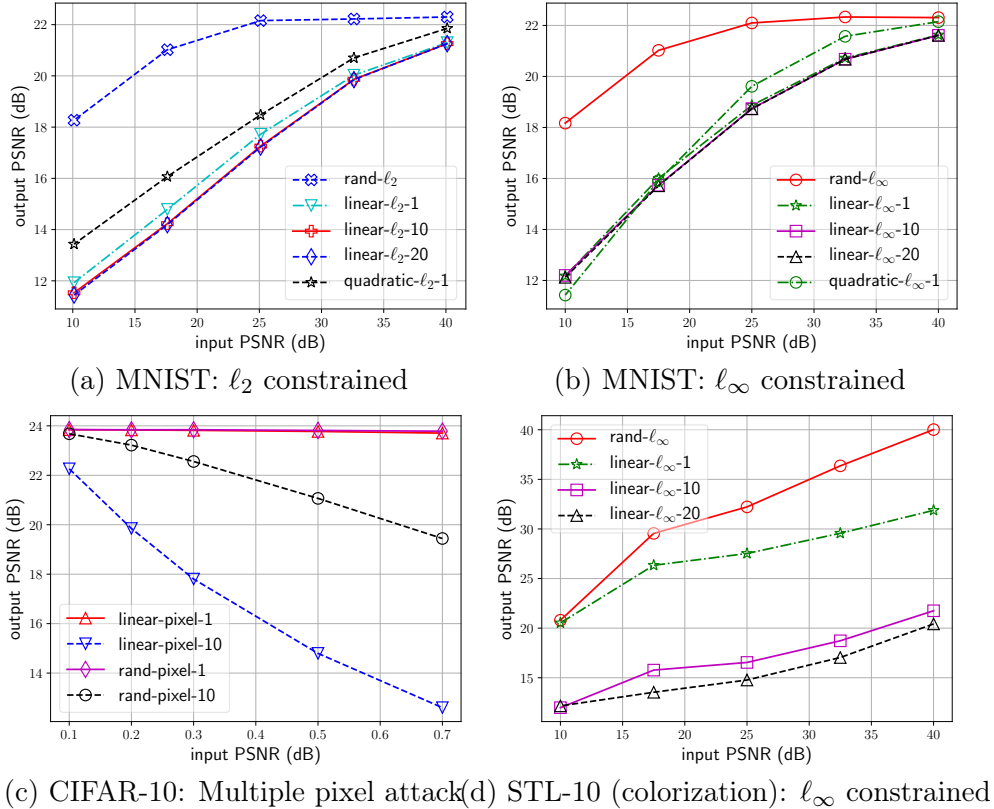


Figure 4: Output PSNR for (a): MNIST autoencoder under ℓ_2 -norm constraint, (b): MNIST autoencoder under ℓ_∞ -norm constraint, (c): CIFAR-10 autoencoder under multiple pixel attacks, (d): STL-10 colorization network under ℓ_∞ -norm constraint.

- **FGSM**: This well-known method was proposed by [GSS14] where $L(\mathbf{x}, \boldsymbol{\eta})$ is replaced by the negative training loss for the input $\mathbf{x} + \boldsymbol{\eta}$. Usually the cross-entropy loss is used for this purpose. With the newly replaced function, (5) is solved for $p = \infty$.
- **PGD**: This method is the iterative version of FGSM ($T > 1$) with $\tilde{\varepsilon}_1 = \varepsilon$ and $\tilde{\varepsilon}_t = 0$ for all $t > 1$. It constitutes one of the state of the art attacks in the literature.
- **DeepFool**: This method was proposed in [MDFF16] and makes use of iterative approximations. Every iteration of DeepFool can be written within our framework by replacing L by

$$L(\mathbf{x}, \boldsymbol{\eta}) = f_{k(\mathbf{x})}(\mathbf{x} + \boldsymbol{\eta}) - f_{\hat{l}}(\mathbf{x} + \boldsymbol{\eta}), \quad \text{where}$$

$$\hat{l} = \operatorname{argmin}_{l \neq k(\mathbf{x})} \left\{ \frac{|f_{k(\mathbf{x})}(\mathbf{x}) - f_l(\mathbf{x})|}{\|\nabla f_{k(\mathbf{x})}(\mathbf{x}) - \nabla f_l(\mathbf{x})\|_q} \right\}.$$

The adversarial perturbations are computed using $p = \infty$, thus $q = 1$, with a maximum of 50 iterations. These parameters were taken from [MDFF16]. Note that \hat{l} is chosen to minimize the robustness $\hat{\rho}_1(f)$ for $\mathcal{D} = \{\mathbf{x}\}$.

- **Random**: For benchmarking purposes, we also consider random perturbations with independent Bernoulli distributed entries with $\mathbb{P}(\varepsilon) = \mathbb{P}(-\varepsilon) = \frac{1}{2}$. This helps to demarcate the essential difference of adversarial and random perturbations.

Note that these methods from the literature can be expressed in terms of the proposed framework as summarized in Table 1. In that table we also include the black-box ensemble attack from

[TKP⁺18] and targeted attacks [CW17, PMJ⁺16, BF17, CANK17, SBMC17]. In [TKP⁺18] the target neural network function is not known thus another known neural network function f is used instead, hoping that the obtained adversarial example transfers to the unknown network. Targeted attacks are used when the objective is to generate adversarial examples that are classified by target system as belonging to some given target class $\ell \in [K]$. That corresponds to fixing the l in (2), that is $L(\mathbf{x}, \boldsymbol{\eta}) = f_{k(\mathbf{x})}(\mathbf{x} + \boldsymbol{\eta}) - f_l(\mathbf{x} + \boldsymbol{\eta})$.

The above methods are tested on the following deep neural network architectures:

- **MNIST** : A fully connected network with two hidden layers of size 150 and 100 respectively, as well as the LeNet-5 architecture [LHBB99].
- **CIFAR-10** : The Network In Network (NIN) architecture [LCY13], and a 40 layer DenseNet [HLWvdM17].

As a performance measure, we use the *fooling ratio* defined in [MDF16] as the percentage of correctly classified images that are missclassified when adversarial perturbations are applied. Of course, the fooling ratio depends on the constraint on the norm of adversarial examples. Therefore, in Figure 3 we observe the fooling ratio for different values of ε on the aforementioned neural networks. As expected, the increased computational complexity of iterative methods such as DeepFool and Algorithm 1- T translates into increased performance with respect to non-iterative methods. Nevertheless, as shown in Figures 3(a) and (c), the performance gap between iterative and non-iterative algorithms is not always significant. For the case of iterative algorithms, the proposed Algorithm 1- T outperforms DeepFool and PGD. The same holds true for Algorithm 1 with respect to other non-iterative methods such as FGSM, while Algorithm 2 obtains competitive performance with respect to FGSM. However, note that adversarial training using PGD is the state of the art defense against adversarial examples, thus PGD may still be a better choice than Algorithm 1- T for adversarial training.

Finally, we measure the robustness of different networks using $\hat{\rho}_1(f)$ and $\hat{\rho}_2(f)$, with $p = \infty$. We also include the minimum ε , such that DeepFool obtains a fooling ratio greater than 99%, as a performance measure as well. These results are summarized in Table 3, where we obtain coherent results between the 3 measures.

| | Test error | $\hat{\rho}_1(f)$ [MDF16] | $\hat{\rho}_2(f)$ (ours) | fooled >99% |
|---------------------|------------|------------------------------|-----------------------------|--------------------------------|
| FCNN (MNIST) | 1.7% | 0.036 | 0.034 | $\varepsilon = 0.076$ |
| LeNet-5 (MNIST) | 0.9% | 0.077 | 0.061 | $\varepsilon = \mathbf{0.164}$ |
| NIN (CIFAR-10) | 13.8% | 0.012 | 0.004 | $\varepsilon = \mathbf{0.018}$ |
| DenseNet (CIFAR-10) | 5.2% | 0.006 | 0.002 | $\varepsilon = 0.010$ |

Table 3: Robustness measures for different classifiers.

6.2 Regression

For the sake of clarity we use the notation *quadratic- ℓ_p* to denote the method of computing adversarial perturbations by solving the quadratic problem (13) under the ℓ_p -norm constraint. In the same manner, Algorithm 1 with T iterations and the ℓ_p -norm constraint is referred to as *linear- ℓ_p - T* . Since the experiments carried out in this section are exclusively image based, we use the notation *linear-pixel- T* to denote the multiple subset attack with $\|\boldsymbol{\eta}\|_{0,S} = T$. Since the aim of the proposed attacks is to maximize the MSE of the target system, we use the Peak-Signal-to-Noise Ratio (PSNR), which is a common measure for image quality and is defined as $\text{PSNR} = (\text{maximum pixel value})^2 / \text{MSE}$, as the performance metric.

Similarly to [MDF16], we show the validity of our methods by comparing their performance against appropriate types of random noise. For $p = 2$ the random perturbation is computed as

$\boldsymbol{\eta} = \varepsilon \mathbf{w} / \|\mathbf{w}\|_2$, where the entries of \mathbf{w} are independently drawn from a Gaussian distribution. For $p = \infty$ the random perturbation $\boldsymbol{\eta}$ has independent Bernoulli distributed entries with $\mathbb{P}(\varepsilon) = \mathbb{P}(-\varepsilon) = 1/2$. In the case of multiple subset attacks we perform the same approach as for $p = \infty$ but only on T randomly chosen pixels, while setting the other pixels of $\boldsymbol{\eta}$ to zero. In order to keep a consistent notation, we refer to these 3 methods of generating random perturbations as *random- ℓ_2* , *random- ℓ_∞* , and *random-pixel- T* respectively. For our experiments we use the MNIST, CIFAR-10 and STL-10 datasets. A different neural network is trained for each of these datasets. As in [TTV16], we also consider autoencoders. For MNIST and CIFAR-10 we have trained fully connected autoencoders with 96% and 50% compression rates respectively. In addition, we go beyond autoencoders and train the image colorization architecture from [BMRG17] for the STL-10 dataset. Different example images obtained from applying the proposed methods on these networks are shown in Figure 2. For instance, in Figure 2(a) we observe that the autoencoder trained on MNIST is able to denoise random perturbation correctly but fails to do so with adversarial perturbations obtained using the *quadratic- ℓ_∞* method. Similarly, in Figure 2(b), the *random-pixel-100* algorithm distorts the output significantly more than its random counterpart. These two experiments align with the observation of [TTV16] that autoencoders tend to be more robust to adversarial attacks than deep neural networks used for classification. The deep neural network trained for colorization is highly sensitive to adversarial perturbations as illustrated in Figure 2(c), where the original and adversarial images are nearly identical.

While the results shown in Figure 2 are for some particular images, in Figure 4 we measure the performance of different adversarial attacks using the average output PSNR over 20 randomly selected images from the corresponding datasets. In Figures 4(a) and 4(b) we observe how computing adversarial perturbations through successive linearizations improves the performance. This behavior is more pronounced in Figure 4(d), where iterative linearizations are responsible for more than 10 dB of output PSNR reduction. Note that, in Figures 4(a) and 4(b) the non-iterative *quadratic- ℓ_p* algorithm performs competitively, even when compared to iterative methods. In Figure 4(b) we observe that the autoencoder trained on CIFAR-10 is robust to single pixel attacks. However, an important degradation of the systems performance, with respect to random noise, can be obtained through adversarial perturbations in the 100 pixels attack ($\approx 9.7\%$ of the total number of pixels). Finally, in Figure 4(d), we can clearly observe the instability of the image colorization network to adversarial attacks. These experiments show that, even though autoencoders are somehow robust to adversarial noise, this may not be true for deep neural networks in other regression problems.

7 Conclusion

The perturbation analysis of different learning algorithms leads to a framework for generating adversarial examples via convex programming. For classification we have formulated already existing methods as special cases of the proposed framework as well as proposing novel methods for designing adversarial perturbations under various desirable constraints. This includes in particular single-pixel and single-subset attacks. The framework is additionally used to demonstrate adversarial vulnerability of regression algorithms by generating adversarial perturbations. We numerically evaluate the applicability of this framework first by benchmarking the newly introduced algorithms for classification through empirical simulations of the fooling ratio benchmarked against the well-known FGSM, DeepFool, and PGD methods. Through experiments we have shown the existence of adversarial examples in regression for the case of autoencoders and image colorization tasks.

References

- [AC18] Anish Athalye and Nicholas Carlini. On the Robustness of the CVPR 2018 White-Box Adversarial Example Defenses. *arXiv:1804.03286 [cs, stat]*, April 2018. arXiv:1804.03286.
- [ACW18] Anish Athalye, Nicholas Carlini, and David Wagner. Obfuscated Gradients Give a False Sense of Security: Circumventing Defenses to Adversarial Examples. In *International Conference on Machine Learning*, 2018.
- [AM18] N. Akhtar and A. Mian. Threat of Adversarial Attacks on Deep Learning in Computer Vision: A Survey. *IEEE Access*, 6:14410–14430, 2018.
- [BBM18] Emilio Rafael Balda, Arash Behboodi, and Rudolf Mathar. On generation of adversarial examples using convex programming. In *52-th Asilomar Conference on Signals, Systems, and Computers*, pages 1–6, Pacific Grove, California, USA, October 2018.
- [BF17] S. Baluja and I. Fischer. Adversarial Transformation Networks: Learning to Generate Adversarial Examples. *arXiv e-prints*, March 2017.
- [BMRG17] Federico Baldassarre, Diego González Morín, and Lucas Rodés-Guirao. Deep koalarization: Image colorization using cnns and inception-resnet-v2. *arXiv preprint arXiv:1712.03400*, 2017.
- [BNJT10] Marco Barreno, Blaine Nelson, Anthony D. Joseph, and J. D. Tygar. The security of machine learning. *Machine Learning*, 81(2):121–148, November 2010.
- [CANK17] Moustapha Cisse, Yossi Adi, Natalia Neverova, and Joseph Keshet. Houdini: Fooling deep structured prediction models. *arXiv preprint arXiv:1707.05373*, 2017.
- [CW17] Nicholas Carlini and David Wagner. Towards evaluating the robustness of neural networks. In *Security and Privacy (SP), 2017 IEEE Symposium on*, pages 39–57. IEEE, 2017.
- [FFF15] Alhussein Fawzi, Omar Fawzi, and Pascal Frossard. Fundamental limits on adversarial robustness. *Proceedings of ICML, Workshop on Deep Learning*, 2015.
- [FMDF16] Alhussein Fawzi, Seyed-Mohsen Moosavi-Dezfooli, and Pascal Frossard. Robustness of classifiers: from adversarial to random noise. In *Advances in Neural Information Processing Systems 29*, pages 1632–1640. 2016.
- [FMDF17] A. Fawzi, S. M. Moosavi-Dezfooli, and P. Frossard. The Robustness of Deep Networks: A Geometrical Perspective. *IEEE Signal Processing Magazine*, 34(6):50–62, November 2017.
- [FR13] Simon Foucart and Holger Rauhut. *A Mathematical Introduction to Compressive Sensing*. Applied and Numerical Harmonic Analysis. Springer New York, New York, NY, 2013.
- [GSS14] Ian J. Goodfellow, Jonathon Shlens, and Christian Szegedy. Explaining and Harnessing Adversarial Examples. In *International Conference on Learning Representations*, December 2014.
- [GW95] Michel X Goemans and David P Williamson. Improved approximation algorithms for maximum cut and satisfiability problems using semidefinite programming. *Journal of the ACM (JACM)*, 42(6):1115–1145, 1995.

- [HA17] Matthias Hein and Maksym Andriushchenko. Formal guarantees on the robustness of a classifier against adversarial manipulation. In *NIPS*, 2017.
- [HDY⁺12] G. Hinton, L. Deng, D. Yu, G. E. Dahl, A. r Mohamed, N. Jaitly, A. Senior, V. Vanhoucke, P. Nguyen, T. N. Sainath, and B. Kingsbury. Deep Neural Networks for Acoustic Modeling in Speech Recognition: The Shared Views of Four Research Groups. *IEEE Signal Processing Magazine*, 29(6):82–97, November 2012.
- [HH15] David Hartman and Milan Hladík. Tight Bounds on the Radius of Nonsingularity. In *Scientific Computing, Computer Arithmetic, and Validated Numerics*, Lecture Notes in Computer Science, pages 109–115. Springer, Cham, September 2015.
- [HJ13] Roger A. Horn and Charles R. Johnson. *Matrix analysis*. Cambridge Univ. Press, Cambridge, 2. ed edition, 2013.
- [HLWvdM17] Gao Huang, Zhuang Liu, Kilian Q Weinberger, and Laurens van der Maaten. Densely connected convolutional networks. In *Proceedings of the IEEE conference on computer vision and pattern recognition*, volume 1, page 3, 2017.
- [HZRS16] K. He, X. Zhang, S. Ren, and J. Sun. Deep Residual Learning for Image Recognition. In *2016 IEEE Conference on Computer Vision and Pattern Recognition (CVPR)*, pages 770–778, June 2016.
- [KFS18] J. Kos, I. Fischer, and D. Song. Adversarial Examples for Generative Models. In *2018 IEEE Security and Privacy Workshops (SPW)*, pages 36–42, May 2018.
- [KGB16] Alexey Kurakin, Ian Goodfellow, and Samy Bengio. Adversarial examples in the physical world. *arXiv preprint arXiv:1607.02533*, 2016.
- [KH09] Alex Krizhevsky and Geoffrey Hinton. Learning multiple layers of features from tiny images. 2009.
- [KSH12] Alex Krizhevsky, Ilya Sutskever, and Geoffrey E Hinton. Imagenet classification with deep convolutional neural networks. In *Advances in neural information processing systems*, pages 1097–1105, 2012.
- [LCB10] Yann LeCun, Corinna Cortes, and CJ Burges. Mnist handwritten digit database. *AT&T Labs [Online]*. Available: <http://yann.lecun.com/exdb/mnist>, 2, 2010.
- [LCY13] Min Lin, Qiang Chen, and Shuicheng Yan. Network in network. *arXiv preprint arXiv:1312.4400*, 2013.
- [LHBB99] Yann LeCun, Patrick Haffner, Léon Bottou, and Yoshua Bengio. Object recognition with gradient-based learning. In *Shape, contour and grouping in computer vision*, pages 319–345. Springer, 1999.
- [LHL⁺17] Yen-Chen Lin, Zhang-Wei Hong, Yuan-Hong Liao, Meng-Li Shih, Ming-Yu Liu, and Min Sun. Tactics of Adversarial Attack on Deep Reinforcement Learning Agents. In *Proceedings of the 26th International Joint Conference on Artificial Intelligence, IJCAI’17*, pages 3756–3762, Melbourne, Australia, 2017. AAAI Press.
- [MDFF16] Seyed Mohsen Moosavi Dezfooli, Alhussein Fawzi, and Pascal Frossard. Deepfool: a simple and accurate method to fool deep neural networks. In *Proceedings of 2016 IEEE Conference on Computer Vision and Pattern Recognition (CVPR)*, 2016.
- [MDFFF17] Seyed-Mohsen Moosavi-Dezfooli, Alhussein Fawzi, Omar Fawzi, and Pascal Frossard. Universal adversarial perturbations. *arXiv preprint*, 2017.

- [MKBF17] Jan Hendrik Metzen, Mummadi Chaithanya Kumar, Thomas Brox, and Volker Fischer. Universal adversarial perturbations against semantic image segmentation. *stat*, 1050:19, 2017.
- [MMS⁺18] Aleksander Madry, Aleksandar Makelov, Ludwig Schmidt, Dimitris Tsipras, and Adrian Vladu. Towards Deep Learning Models Resistant to Adversarial Attacks. In *International Conference on Learning Representations*, 2018.
- [PMJ⁺16] Nicolas Papernot, Patrick McDaniel, Somesh Jha, Matt Fredrikson, Z Berkay Celik, and Ananthram Swami. The limitations of deep learning in adversarial settings. In *Security and Privacy (EuroS&P), 2016 IEEE European Symposium on*, pages 372–387. IEEE, 2016.
- [PMSH16] Nicolas Papernot, Patrick McDaniel, Ananthram Swami, and Richard Harang. Crafting adversarial input sequences for recurrent neural networks. In *Military Communications Conference, MILCOM 2016-2016 IEEE*, pages 49–54. IEEE, 2016.
- [PMW⁺16] Nicolas Papernot, Patrick McDaniel, Xi Wu, Somesh Jha, and Ananthram Swami. Distillation as a defense to adversarial perturbations against deep neural networks. In *Security and Privacy (SP), 2016 IEEE Symposium on*, pages 582–597. IEEE, 2016.
- [RHGS17] S. Ren, K. He, R. Girshick, and J. Sun. Faster R-CNN: Towards Real-Time Object Detection with Region Proposal Networks. *IEEE Transactions on Pattern Analysis and Machine Intelligence*, 39(6):1137–1149, June 2017.
- [Roh00] Jiří Rohn. Computing the norm $\|A\|_{\infty,1}$ is NP-hard. *Linear and Multilinear Algebra*, 47(3):195–204, May 2000.
- [RRN12] Nikhil Rao, Ben Recht, and Robert Nowak. Universal Measurement Bounds for Structured Sparse Signal Recovery. In *Artificial Intelligence and Statistics*, pages 942–950, March 2012.
- [RSL18] Aditi Raghunathan, Jacob Steinhardt, and Percy Liang. Certified Defenses against Adversarial Examples. In *International Conference on Learning Representations*, 2018.
- [SBMC17] Sayantan Sarkar, Ankan Bansal, Upal Mahbub, and Rama Chellappa. Upset and angry: Breaking high performance image classifiers. *arXiv preprint arXiv:1707.01159*, 2017.
- [SLJ⁺15] Christian Szegedy, Wei Liu, Yangqing Jia, Pierre Sermanet, Scott Reed, Dragomir Anguelov, Dumitru Erhan, Vincent Vanhoucke, and Andrew Rabinovich. Going deeper with convolutions. In *Proceedings of the IEEE Conference on Computer Vision and Pattern Recognition*, pages 1–9, 2015.
- [SVK17] Jiawei Su, Danilo Vasconcellos Vargas, and Sakurai Kouichi. One pixel attack for fooling deep neural networks. *arXiv preprint arXiv:1710.08864*, 2017.
- [SZS⁺14] Christian Szegedy, Wojciech Zaremba, Ilya Sutskever, Joan Bruna, Dumitru Erhan, Ian Goodfellow, and Rob Fergus. Intriguing properties of neural networks. *International Conference on Learning Representations*, 2014.
- [TG16] Thomas Tanay and Lewis Griffin. A Boundary Tilting Perspective on the Phenomenon of Adversarial Examples. *arXiv:1608.07690 [cs, stat]*, August 2016. arXiv: 1608.07690.

- [TKP⁺18] Florian Tramèr, Alexey Kurakin, Nicolas Papernot, Ian Goodfellow, Dan Boneh, and Patrick McDaniel. Ensemble Adversarial Training: Attacks and Defenses. In *International Conference on Learning Representations*, 2018.
- [TSE⁺18] Dimitris Tsipras, Shibani Santurkar, Logan Engstrom, Alexander Turner, and Aleksander Madry. Robustness May Be at Odds with Accuracy. *arXiv:1805.12152 [cs, stat]*, May 2018. arXiv: 1805.12152.
- [TTV16] Pedro Tabacof, Julia Tavares, and Eduardo Valle. Adversarial images for variational autoencoders. *arXiv preprint arXiv:1612.00155*, 2016.
- [WGQ17] Beilun Wang, Ji Gao, and Yanjun Qi. A Theoretical Framework for Robustness of (Deep) Classifiers against Adversarial Examples. In *International Conference on Learning Representations*, 2017.
- [XWZ⁺17] Cihang Xie, Jianyu Wang, Zhishuai Zhang, Yuyin Zhou, Lingxi Xie, and Alan Yuille. Adversarial examples for semantic segmentation and object detection. In *International Conference on Computer Vision. IEEE*, 2017.